JOC The Journal of Organic Chemistry

pubs.acs.org/joc Featured Article

Pseudodiproline (Pro−Cyp) Oligomers Fold into Helical Polyproline Type secondary structures

Jean-Baptiste Garsi, Pedro M. Aguiar, Gilles Berger, Thierry Maris, and Stephen Hanessian*

Cite This: J. Org. Chem. 2024, 89, 4283−4293 Read Online

ACCESS | Metrics & More | Article Recommendations | Supporting Information

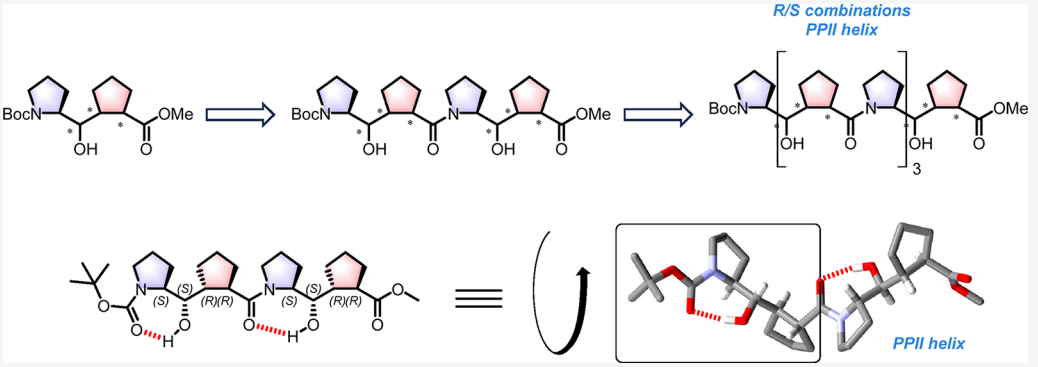

ABSTRACT: The synthesis and conformational properties of oligo-proline mimetics composed of dimeric and tetrameric Pro−Cyp constructs linked by a hydroxymethylene unit are reported. Oligomers were studied both in the solid state and in solution, unveiling right-handed helical conformation depending on the configuration of the vicinally substituted *trans*-cyclopentane carboxylic acid unit (Cyp). Unlike polyproline oligomers, the alternating synthetic Pro−Cyp counterparts are not stabilized by $n-\pi^*$ interactions but rely instead on the steric demands of the extended backbone conformation within the hydroxymethylene-linked Pro−Cyp repeating units.

INTRODUCTION

The quest to mimic the 3-dimensional helical structure of polyprolines has been a time-tested endeavor over the years.[1−7] The structural requirements for such motifs depend on, among others, the most thermodynamically stable conformation of the oligomeric units which satisfies spatial, structural, and stereoelectronic properties.[7,8] Polyprolines can fold into three-dimensional arrays known as polyprolines I (PPI) and II (PPII), differing in their length and sense of helicity. As a left-handed helix, polyproline II is found in a plethora of proteins, as for example, the structural protein collagen.[8−11] Several examples were crystallized, revealing the three-dimensional geometry of the conformation.[12,13] Scholarly work by Raines and others has laid a strong foundation for our understanding of the importance of the conformation of collagen and synthetic mimics comprising substituted prolines in relation to their function.[1,2,8,14−17] As an example, the triple helix structure encompassing a PPII motif was mimicked in the X-ray crystal structure of a model $[(Pro-Pro-Gly)_{10}]_3$ oligo-proline.[18] Efforts to obtain short oligo-proline units as truncated PPII-type surrogates have been limited mainly to the study of their conformations by circular dichroism.[19−21] Securing single crystals of small polyproline oligomers suitable for X-ray structural analysis has remained elusive over the years. In 2014, Wennemers successfully obtained a crystal structure of a proline hexamer as the N-terminal *p*-bromo benzamide derivative exhibiting a PPII helical conformation.[22] This study provided valuable insights regarding the conformation of a hexa-proline unit as a PPII helix in the absence of hydrating water molecules (Figure 1a). Some oligo-prolines have revealed added benefits for biological or materials applications.[23,24]

To the best of our knowledge, the shortest oligo-proline core structure to adopt a left-handed PPII-type helical conformation in the crystalline state is a tetramer of 4,5-*cis*-methano-L-proline methyl ester hydrochloride[25] (Figure 1A). Its X-ray structure, DFT-optimized calculations, and NBO analysis indicate that each residue participates in a strong $n-\pi^*$ interaction for a total stabilization energy of 3.0 kcal mol^{-1}. As few as three *cis*-4,5-methano-L-proline units showed progression toward a helical folding pattern. The corresponding *trans*-4,5-methano-

Received: December 12, 2023
Revised: March 3, 2024
Accepted: March 11, 2024
Published: March 15, 2024

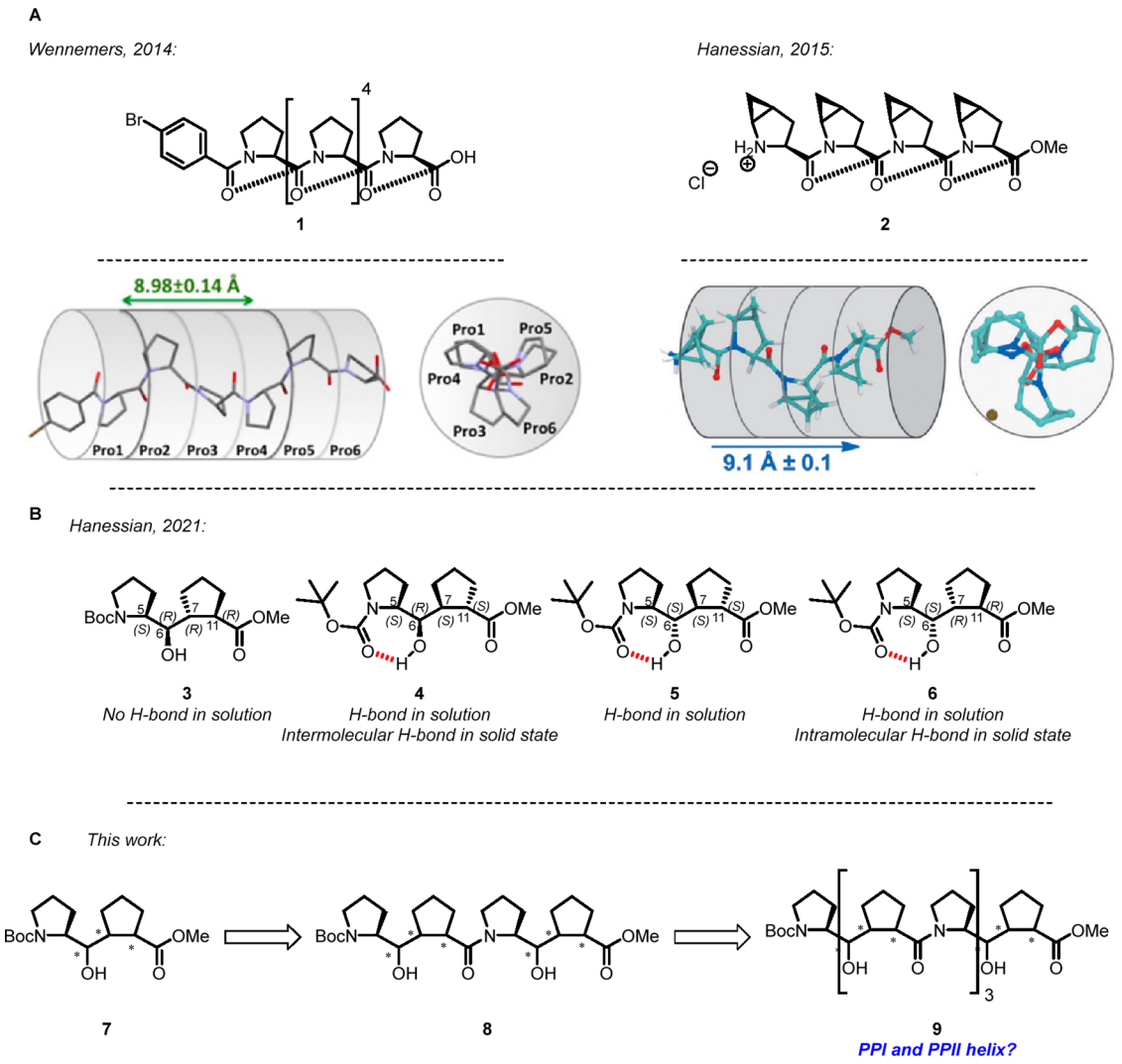

Figure 1. A. Crystallized hexameric polyproline PPII-helix **1** by Wennemers. Reproduced from ref 22. Copyright 2014 American Chemical Society. Shortest tetrameric *cis*-4,5-methanoproline **2** by Hanessian. Reproduced from ref 25. Copyright 2015 John Wiley and Sons. B. Structure and characteristic H-bonding patterns observed in solution and solid-state for pseudodiproline Pro−Cyp surrogates **3**−**6**. C. Generic structure of the Pro−Cyp monomer **7**, dimer **8**, and tetramer **9**. * = stereogenic carbon.

L-proline did not benefit from the same hyperconjugative stabilization and remained disordered.

In a previous report, we described methodologies for the stereocontrolled synthesis of diastereomeric pseudodiproline units **3**−**6** designated as "Pro−Cyp" consisting of an α-pyrrolidinyl residue linked to a *trans*-1,2-cyclopentane carboxylic acid by a stereochemically defined hydroxymethylene tether[26] (Figure 1B). The cyclopentane ring in such Pro−Cyp units was intended as a carbocyclic structural substitute for a proline residue with an *R*- or *S*- configured methine hydroxyl group replacing the carbonyl group of the original Pro−Pro amide bond. Thus, an oligomeric Pro−Cyp construct would consist of alternating units of hydroxymethyl-linked α-pyrrolidinyl 1,2-*trans*-cyclopentane carboxylic acid amides of predetermined absolute stereochemistry. As a proof-of-concept, we first tested the validity of replacing oligo-proline units with a Pro−Cyp surrogate in a challenging medicinally relevant target.[27] The native amino acid sequence in the cytosolic p22phox protein contains a "hot spot" encompassing a Pro−Pro−Pro unit which is recognized by the regulatory p47 protein, resulting in the activation of the enzyme NADPH oxidase (NOX) which is involved in the production of reactive oxygen species (ROS). A truncated synthetic version of p22phox modified at the N-and C-termini and containing the same triproline sequence was an active inhibitor in the submicromolar range (K_i = 0.2 μM). Replacement of the Pro−Pro−Pro "hot spot" by a Pro−Pro−Cyp unit in the same truncated analogue revealed promising inhibitory activity against NOX. Replacement of the same triproline segment with the alternative Pro−Cyp−Pro unit led to an inactive analogue, which indicated that the Cyp unit in the active analogue acted as a structurally favorable molecular substitute for the third proline unit in the truncated p22 analogue. In another example, replacing Thr32 and Gln34 in the C-terminal Neuropeptide Y fragment 25−36 by a *cis*-cyclopentane β-amino acid shifted the selectivity toward the receptor.[28]

Inclusion of cyclopentane rings in diverse oligomeric constructs has resulted in helical structures. For example, *R,R*- or *S,S*-1,2-amino cyclopentane carboxylic acids have been used in conjunction with the design of helical peptidic foldamers.[29] Alternating amides of *R,R*- or *S,S*-*trans*-1,2-diaminocyclopentane with 2,2-dimethyl malonic acid led to

https://doi.org/10.1021/acs.joc.3c02840
J. Org. Chem. 2024, 89, 4283−4293

Scheme 1. A. Representative Example of the Synthetic Approach toward Pro−Cyp Dimers 14−17 (12 = 14) and Tetramers 22−25 (13 = 22) from Pro−Cyp Monomers 3−6. B. Structures of Pro−Cyp Dimers 14−17 (12 = 14) and Tetramers 22−25 (13 = 22)

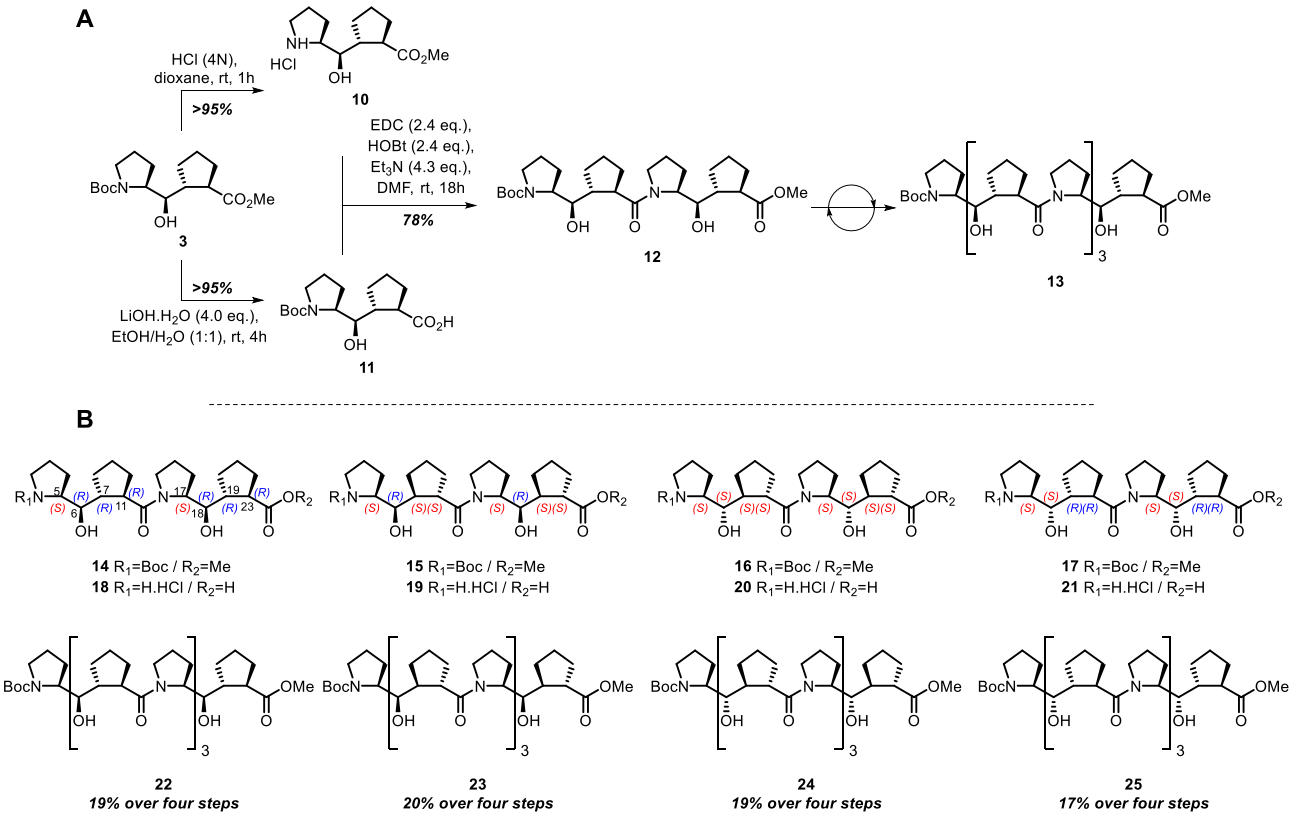

left- and right-handed helical structures.[30] Cyclopentane nucleic acid peptides fold into helices that are recognized by DNA.[31]

To consider the engineering of polyproline mimetics with Pro−Cyp units as a molecular substitute for Pro−Pro−X sequences in general, it is necessary to first study the solution and solid-state structures and conformations of the corresponding oligomers. Unlike polyprolines, Pro−Cyp oligomers cannot benefit from $n-\pi^*$ hyperconjugative stabilization.[23,25] Nonetheless, we hoped that the combination of intramolecular H-bonding from the *R*- or *S*-methine hydroxyl groups with the proline amide carbonyl groups, coupled with the stereochemistry of the *trans*-1,2-substituted cyclopentane carboxamide in Pro−Cyp oligomers would fold into helical structures. There remained to determine which of the above parameters if any was important in achieving a conformationally stable helical structure.

Herein, we describe the synthesis of four stereochemically distinct Pro−Cyp dimers (diads) and tetramers (tetrads) to probe their three-dimensional conformations as pseudodiproline mimetics of polyproline I and polyproline II-like structures.

RESULTS AND DISCUSSION

Synthesis. The synthesis was accomplished through a series of iterative amide couplings of Pro−Cyp units which were either subjected to removal of the N-Boc protective group or to hydrolysis of the methyl ester. One and two-directional amide coupling of the individual Pro−Cyp units delivered homodimers **14**−**17** (Scheme 1A). These were converted to the corresponding amino acids **18**−**21** (Scheme 1B). Following the same protocol, the dimers were converted to the corresponding N-Boc methyl ester tetramers **22**−**25**, which were obtained in high purity after separation by preparative high-performance liquid chromatography (see Supporting Information).

Conformations in the Solid State. In our previous report,[26] an X-ray structure of the N-Boc Pro−Cyp methyl ester **6** corresponding to a 6*S*,7*R*,11*R* configuration revealed the presence of a hydrogen bond between the carbonyl of the Boc and the methine hydroxyl group at C6 similar to a γ-turn in a regular dipeptide (Figure 2B). This observation led us to anticipate that the corresponding dimer **17** would exhibit a second seven-membered ring hydrogen bond, now with the proline amide carbonyl group. Our expectation was confirmed from an X-ray analysis of a single crystal of dimer **17** (recrystallized from CH_2Cl_2) (Figure 2). Indeed, a hydrogen bond was formed between the N-carbonyl and the C6 *S*-configured hydroxyl group of each monomeric Pro−Cyp unit. More pleasingly, the backbone conformation encompassing C5 to C11 and repeating with C17−C23 of two *trans*-1,2-cyclopentane rings with a 7*R*,11*R* configurations in dimer **17** adopted an extended left-handed helix shape composed of three Pro−Cyp−Pro residues per turn. Unfortunately, the dimer **15** obtained from **4**[26] did not crystallize.

The crystal of dimer **17** was found in an *I*2 space group, and no symmetry axis was observed since it consisted of only two Pro−Cyp monomers for an *n*+3 helix. The pitch measured from Pro1 to Cyp2 was 9.6 Å, with distances between adjacent residues averaging 3.3 Å (see Figure S1) which is analogous

https://doi.org/10.1021/acs.joc.3c02840
J. Org. Chem. 2024, 89, 4283−4293

A

Ring	ω (°)	ϕ (°)	ψ (°)	Pucker
A (Pro1)	-	-82.2	-175.7	C^{γ}-exo (C3)
B (Cyp1)	180.0	-83.8	178.1	C^{δ}-exo (C8)
C (Pro2)	-165.5	-79.4	-167.5	C^{γ}-exo (C15)
D (Cyp2)	-176.7	-103.3	-	Twisted C^{γ}-exo–C^{δ}-endo (C21-C20)

B

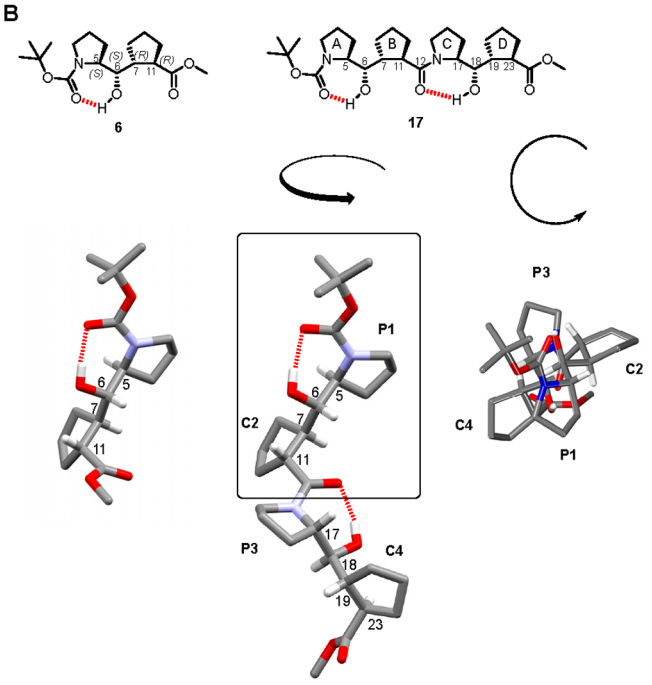

Figure 2. A. Torsion angles of **17** and ring puckers. B. 3-Dimensional representations of the X-ray structures for Pro–Cyp monomer **6** and Pro–Cyp dimer **17**.

from the natural 3.2 Å found in natural polyproline II. Both hydrogen bonds were evidenced by locating the hydrogen atom positions in the electron density difference map (see Supporting Information). The A–C rings in the helix adopt an *exo*-pucker conformation, while ring D has a twisted C^{γ}-*exo*–C^{δ}-*endo* conformation. All torsion angles (ω, ϕ, ψ) were consistent with those observed in an extended PPII conformation with an *exo*-pucker.[32] (Figure 2, Figure S2) ω angles were found in the 180° region, and ϕ angles were located in the low values observed for *exo*-prolines (−80° to −100°). The ϕ angle of Cyp2 was found at −103.3°, which is also in the expected range for twisted prolines. The rings A–C ψ values averaged 170–180°, which is higher than what has been commonly observed for PPII conformations (120–160° for prolines with an *exo*-pucker).[32] ϕ and ψ values indicated that **17** adopted a more extended conformation compared to an ideal PPII helix, especially in the context of *exo* ring pucker residues.

Conformations in Solution. To better understand the tendency of the intended Pro–Cyp oligomers to adopt a helical conformation, we first analyzed the NMR spectra of monomer **6**,[26] the results of which could be extended to oligomers **17** and **25**. In our previous study, we showed that the intramolecular hydrogen-bond found in **6** was maintained in $CDCl_3$.[26] Here, we investigated the torsional angles OH–H6, H5–H6 and H7–H6 in solution for **6**. If comparable values to the ones observed in the solid state were observed, it would be reasonable to assume that a similar conformation could be found in solution. Scalar coupling to the C6 hydrogen (^3J(OH, H6) = 3.3 Hz) at 298 K in $CDCl_3$ was measured, while the OH line width indicated possible dynamics. The H5 and H6 signals were similarly broader, thus preventing measurement of ^3J(H5, H6) and ^3J(H6, H7). Low-temperature experiments were then conducted in an intent to slow dynamics and improve resolution. Upon cooling to 273 K, all the ^{1}H signals significantly sharpened, and coupling constants remained consistent down to 223 K (Figure 3;

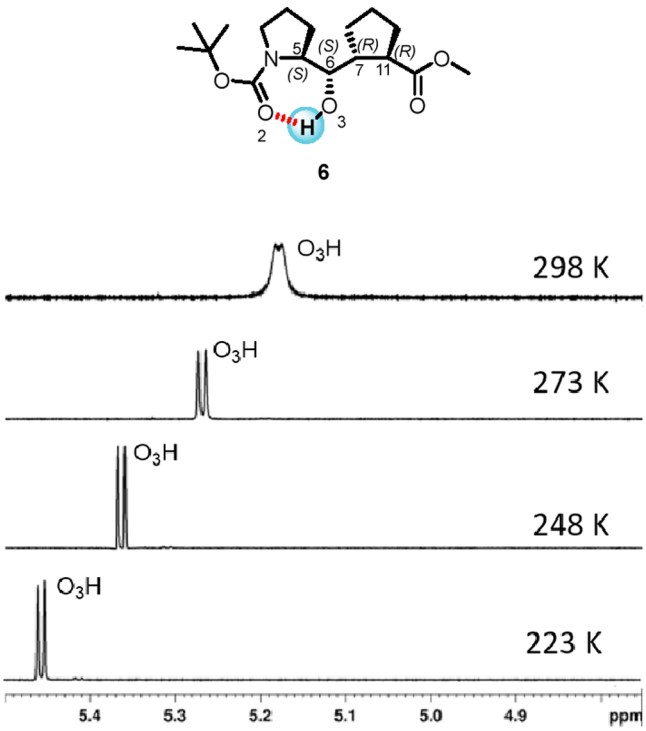

Figure 3. ^{1}H NMR spectra of **6** in $CDCl_3$ at temperatures from 298 to 223 K focusing on the O3–H hydrogen. NB: Spectra were processed with Lorentz–Gaussian resolution-enhancement apodization (lb = −1 Hz, gb = 0.5).

Figure S3). The O3–H shifted downfield upon cooling, as expected for increasing H-bonded character. Using Karplus relations for the torsional angles,[33] the magnitude of the observed *J*-couplings at 223 K in $CDCl_3$ was consistent with the torsional angles observed from single-crystal X-ray diffraction studies, indicating a similar conformation in solution (Table 1).

To probe the importance of the H-bond on the conformational stability of the monomer **6**, the ^3J-couplings were measured in a hydrogen-bond disrupting solvent (DMSO-d_6). At 298 K, the ^{1}H NMR showed a broad OH signal with no visible *J*-coupling, indicative of dynamic exchange and loss of

Table 1. Comparison of ^3J-Coupling Constants of H6 in the Solid-State and in Solution

	X-ray dihedral angle (Estimated ^3J (Hz))	^3J 223 K ($CDCl_3$, Hz)	^3J 388 K (DMSO-d_6, Hz)
OH–H6	102.8° (2.0)	4.0	–
H5–H6	56.5° (2.0)	2.1	2.5
H7–H6	−178.1° (10.3)	10.0	7.7

https://doi.org/10.1021/acs.joc.3c02840
J. Org. Chem. 2024, 89, 4283–4293

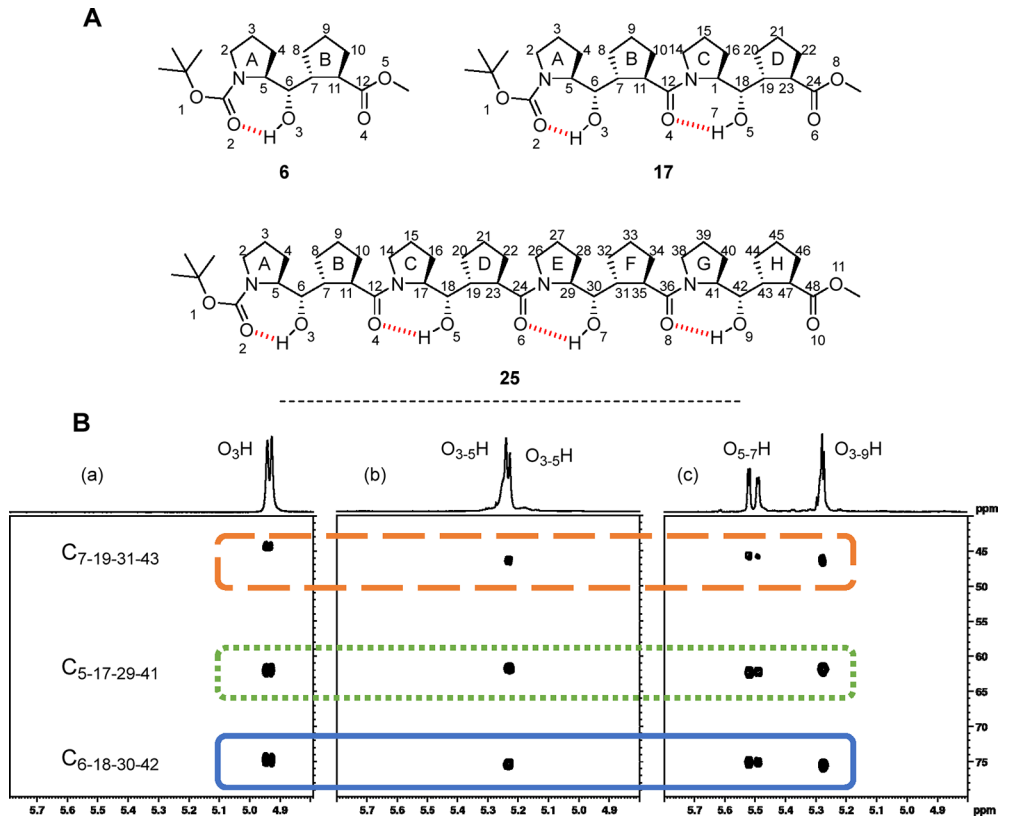

Figure 4. A. Structures of monomer **6**, dimer **17**, and tetramer **25**. B. (a) Hydroxyl $^{1}H-^{13}C$ multiple-bond correlation for monomer **6** (251 K, $CDCl_3$). (b) Hydroxyls $^{1}H-^{13}C$ multiple-bond correlation for dimer **17** (298 K, $CDCl_3$). (c) Hydroxyls $^{1}H-^{13}C$ multiple-bond correlation for tetramer **25** (298 K, $CDCl_3$).

the hydrogen bond (see Figure S4 and S5). The signals of H5 and H6 were equally broad, and the resolution was not conducive to dihedral angle measurement. A set of ^{1}H NMR spectra were recorded at increased temperature to free the structure from dynamic restriction. Upon gradual heating, the resolution of the spectra increased and the ^{3}J-couplings between H6 and its neighbors (H5 and H7) were measured at 388 K. Minimal variation in the angles from those observed at 223 K in $CDCl_3$ was observed, indicating similar dihedral angles despite the possibility for free-rotation about both carbon−carbon bonds (Table 1). Considering that the same backbone restrictions are in play in isomers **3**−**5**, it seems reasonable to suggest that their conformation is also dictated by torsion angles regardless of their propensity for H-bonding. As for monomers **3**−**6**, both dimers' and tetramers' intramolecular H-bonding was disrupted in protic solvent.[26]

With the above solution and solid-state data in hand for monomer **6** as a prototype for extended oligomers, we next studied the solution conformations of the dimer **17** and tetramer **25**, respectively. From the crystal structure of **17**, it was evident that backbone carbon atoms comprising C5−C11 and its repeat unit C17−C23 preferred a quasi-extended conformation encompassing the *trans*-1,2-cyclopentane ring with a 7*R*,11*R* configuration and resulting in a left-handed helical conformation. It was reasonable to assume that the same trend would be observed in the tetramer **25**, which was corroborated with ^{1}H and ^{13}C NMR measurements.

The overlap of the very similar signals from the individual repeat units precluded extraction of accurate *J*-couplings in **17** and **25**. The chemical shifts of the hydroxyl groups were retained in **17** and **25**, indicating that H-bonding was maintained in each repeating Pro−Cyp unit. Within a secondary structure, it is often found that external residues are less ordered than internal repeats due to their exposure to the solvent. We therefore hypothesized that the internal hydrogen bonds between the hydroxyl groups and the amide carbonyl in the repeating Pro−Cyp units of **17** and **25** should be slightly more stabilized compared to the one with the N-Boc group in a stable helical conformation. To probe this property, we analyzed $^{1}H-^{13}C$ multiple-bond correlation (HMBC) NMR in search of differentiation between the individual hydroxyl groups. Taking **6** as a reference, the fluxionality of the OH to carbonyl H-bond was sufficient that no long-range $^{1}H-^{13}C$ correlations could be observed by NMR at room temperature (298 K). At lower temperature (251 K), the H-bonded conformation of the monomer **6** was stabilized enough so that $^{1}H-^{13}C$ multiple-bond correlation signals could be observed from the OH hydrogen and carbons 5, 6, and 7 (located at 3, 2, and 3-bonds away, respectively, from O_3H, Figure 4B(a)). For the dimer **17**, O_3H and O_5H showed distinct behaviors. While the broad O_3H signal yielded no correlations as per in **6**, HMBC correlations were readily observable for O_5H (298 K), indicative of a stronger H-bond (Figure 4B(b)). In addition, the thermal ellipsoid of the O_2 (carbonyl oxygen of **6** Boc group) is larger than the thermal ellipsoid of O_4 (see Supporting Information), indicating greater motion even at 100 K. This is indicative of a weaker interaction to the O_3H hydrogen. For the tetramer **25**, the corresponding HMBC correlations were readily observable for three of the four signals arising from $O_{5-7-9}H$ sites at room temperature (298 K). The fourth O_3H signal yielded no correlations, consistent with the fact that this OH is involved in

https://doi.org/10.1021/acs.joc.3c02840
J. Org. Chem. 2024, 89, 4283−4293

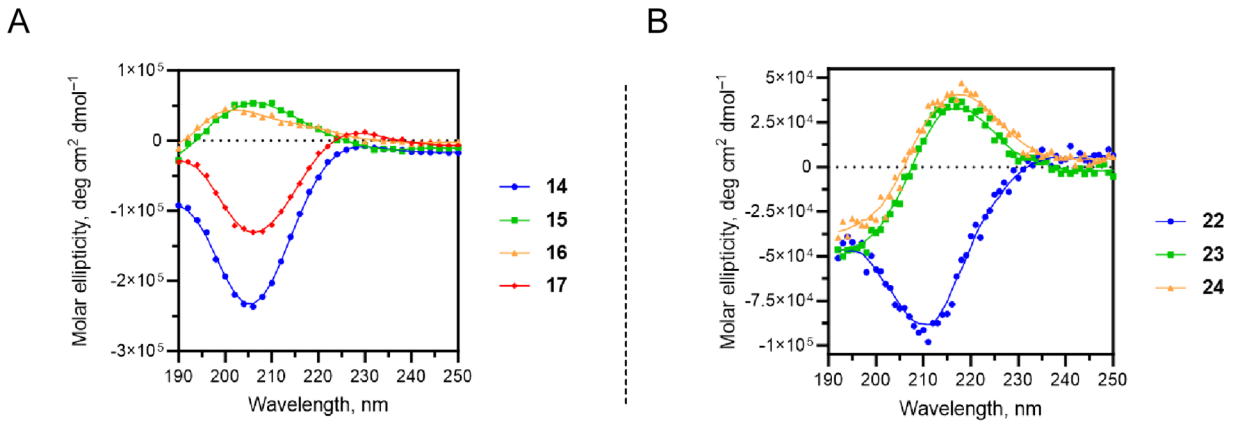

Figure 5. A. ECD of dimers **14**−**17** in a PBS solution. B. ECD of tetramers **22**−**24** in a PBS solution.

the weaker H-bond with the N-Boc group. The hydrogens O_5H and O_7H located in the internal repeating units were shifted downfield compared to O_3H and O_9H, indicating that their H-bonds were strengthened. Taken together, these results, and the pattern observed for hydroxyl groups found in **6**, **17**, and **25** corroborates the hypothesis that a left-handed helical conformation is maintained in the series.

In our previous report describing the Pro−Cyp unit, we observed that the strength of the H-bond was of the same order in isomers **5** and **6** bearing a C6-(*S*) hydroxyl group.[26] We anticipated that if a polyproline conformation was also present in dimer **16** and tetramer **24**, the pattern of the hydroxyl groups found within these structures would be comparable to **17** and **25**. Indeed, a trend similar as in the **6**−**17**−**25** series was observed in the chemical shifts of the hydroxyl groups belonging to the **5**−**16**−**24** series. The chemical shifts for $O_{5-7}H$ and $O_{3-9}H$ in **24** were found at 5.35 and 5.2 ppm, respectively, with the analogous $^1H-^{13}C$ multiple bond correlations found in **25** (see Figures S6−S8). In tetramers **24** and **25**, hydrogens from repeating Pro−Cyp units B−G found in the core of the secondary structure overlapped, consistent with the presence of a helical conformation in which all units share a similar magnetic environment (see Figure S9). The signals for the hydrogens of the end-units A and H were shifted upfield in both **24** and **25**, with comparable variation in their chemical shifts. Taken together, these observations corroborate the hypothesis that **24** adopts a helical conformation as for **25**.

Because Pro−Cyp monomers **3** and **4** carrying a C6-(*R*) hydroxyl group showed weak to no H-bonding, the resolution of the hydroxyls in their dimers and tetramers was affected, preventing our ability to extract the same information in the HMBC spectra as with the **5** and **6** series. However, as for **24** and **25**, hydrogen signals from the core units B−G in **22** and **23** overlapped, whereas those from units A and H were shifted upfield, suggesting the presence of ordered helical structures.

The adoption of a PPII conformation in $CDCl_3$ is a departure from the solvent dependency of natural prolines to adopt PPII conformation. Polyprolines require carbonyl solvation for proper folding, whereas Pro−Cyp oligomers secondary structures are reliant on steric effects. This allows Pro−Cyp oligomers to fold into their secondary structure in organic solvents.

Electronic Circular Dichroism (ECD). Extensive studies have been reported over the years to correlate the conformations of polypeptides such as polyproline I- and polyproline II-types according to their ECD spectral characteristics.[34−36] It is generally accepted that the secondary structures within polyprolines found in proline-rich segments with *trans*-amide bonds fold as left-handed helices corresponding to a PPII-type conformation showing a strong negative band at 205 nm and a weaker positive band at 225 nm.[37,38] Type I polyprolines consist of *cis*-amide bonds that adopt a right-handed helix and exhibit an ECD spectrum in water (pH = 7.5) characterized by a strong negative band at 199 nm, a positive band at 214 nm, and a weak negative band at 230 nm. These values may change depending on external factors such as the nature of the solvent.[39,40] We were curious to know if the replacement of a carbocycle in place of a proline in short Pro−Pro oligomers as in the corresponding Pro−Cyp oligomers would exhibit ECD spectra resembling the characteristic patterns of PPI or PPII in solution.

The spectrum of dimer **17** was recorded in a phosphate buffer solution (PBS, pH = 7) at a concentration of 0.1 mM. An intense negative band was found at ca. 206 nm and a weak positive band at ca. 228 nm, as observed in native oligomers of polyproline II (Figure 5A).[38]

Dimer **14**, with the opposite *R*-configurations at the hydroxyl-bearing methine carbon compared to dimer **17**, exhibited a more pronounced negative band at ca. 205 nm and the absence of a positive band. As for its progenitor **14**, tetramer **22** exhibited a negative band with a slight shift to 210 nm, which is reminiscent of a PPII-like conformation for synthetic variants of polyprolines.[41] Unfortunately, the spectrum of **25** was not recorded due to its poor solubility. Considering that tetramer **25** is derived from its dimeric progenitor **17** of confirmed structure, stereochemistry and sense of helicity, it could be safely assumed that it too adopts a PPII-type helical structure. Dimers **15** and **16** possess a 7*S*,11*S*,19*S*,23*S* configuration in the *trans*-1,2-substituted cyclopentane rings, whereas **14** and **17** have the opposite 7*R*,11*R*,19*R*,23*R* configurations. Dimers **15** and **16** showed a medium-intensity positive band at ca. 206 nm and ca. 200 nm (Figure 5A). The ECD spectra of the corresponding tetramers **23** and **24**, respectively, showed strong positive bands that were shifted to 215 nM. Although a negative band at ca. 190 nm and an intense positive band at ca. 215 nm can be indicative of a PPI-type helix (Figure 5B),[7,39,40] further investigation is needed at that time to assert the secondary structure of these isomers. Given the observed opposite signs in the ECD spectra of the Pro−Cyp tetramers **22** and **23**/**24** regardless of the configuration of the methine carbon in the

https://doi.org/10.1021/acs.joc.3c02840
J. Org. Chem. 2024, 89, 4283−4293

linker, adopting helical conformations in solution for sets of Pro−Cyp oligomers (and in the solid state exemplified by **17**), is inherent to the backbone conformations and absolute configurations of the *trans*-1,2-substituted cyclopentane ring, possibly further stabilized by consequential intramolecular H-bonding from the methine hydroxyl group. Based on the shapes and signs of the ECD spectra, the Pro−Cyp oligomers may qualitatively approximate the conformations of local Pro−Pro structures in longer oligomers. To probe the importance of the influence of the N-Boc group in the dimers **14** − **17**, the ECD spectra of the corresponding amino acid hydrochlorides were measured (see Figure S10). Not surprisingly, no signals were observed, indicating that the N-Boc and methyl ester extremities participate in the stability of the helices.

CONCLUSIONS

We described the synthesis of a series of extended oligomers from diastereomeric Pro−Cyp monomers possessing a *trans*-1,2-substituted cyclopentane unit linked to a proline unit with a hydroxymethylene linker of known configuration. Based on X-ray diffraction studies of dimer **17**, and ECD spectra of other congeners, we showed that tetrameric Pro−Cyp units could adopt natural PPII-like helical conformations which are retained in $CDCl_3$ solution. Notably, we have shown that the configuration of the alternating 1,2-*trans*-cyclopentane carboxylic acid unit in Pro−Cyp oligomers is directly responsible for the tendency to adopt a PPII-like helical conformations. Because one amide bond is replaced by a hydroxy methine linker, Pro−Cyp oligomers may be less prone to *cis*/*trans* isomerization compared to natural polyproline. Strategic incorporation of oligo Pro−Cyp motifs of predetermined length and helicity to replace existing oligo-proline units within biologically relevant polyproline peptides may prove to be of interest in the pursue of protein−protein interaction ligands.[27,42]

EXPERIMENTAL SECTION

General Methods. All reactions were performed in flame-dried glassware under a positive pressure of dry, oxygen-free argon and in dry solvents. All flasks were flushed with three alternative cycles of vacuum/argon and sealed with Teflon. Anhydrous solvents were distilled under a positive pressure of argon before use and dried by standard methods. THF, ether, CH_2Cl_2, and toluene were dried by the SDS (Solvent Delivery System). Commercial-grade reagents were used without further purification. Silica column chromatography was performed on 230−400 mesh silica gel. Reactions were monitored by mass spectrometry with positive ionization or by thin-layer chromatography carried out on a 0.25 mm aluminum-backed plate. Visualization was done by UV light (254 nm) or by staining with potassium permanganate solution, cerium ammonium molybdate (CAM), *p*-anisaldehyde, or ninhydrin solution followed by heating. ^{1}H NMR and 13C{1H} NMR spectra were recorded on Brüker instruments with field strengths notated in the text at room temperature (298 K) with complete proton decoupling for nuclei other than ^{1}H unless otherwise stated. Chemical shifts are reported in parts per million (ppm) referenced from $CDCl_3$ (δ_H: 7.26 ppm and δ_C: 77.0 ppm) and CD_3OD (δ_H: 3.31 ppm and δ_C: 49.0 ppm). Coupling constants (J) are reported in Hertz (Hz). Multiplicities are given as multiplet (m), singlet (s), doublet (d), triplet (t), quartet (q), quintet (quin.), and broad (br.). Optical rotations were determined on an Anton Paar MCP 100 polarimeter at 589 nm at 25 °C. Specific rotations are given in units of 10^{-1} deg cm^2 g^{-1}. High-Resolution Mass Spectra (HRMS) and High-Performance Liquid Chromatography (HPLC) were performed by the "Centre régional de spectroscopie de masse de l'Université de Montréal" with electrospray ionization (ESI) coupled to a quantitative time-of-flight (TOF) detector. Infrared spectra were recorded on an FT-IR spectrometer and are reported in reciprocal centimeters (cm^{-1}). The data for the two crystals were collected from a shock-cooled single crystal at 100 K on a Bruker Smart APEX three-circle diffractometer with a Microfocus Source using Quazar MX Mirror Optics as monochromator and a Bruker APEX2 CCD detector. The diffractometer was equipped with an Oxford Cryostream 700 low-temperature device and used Cu Kα radiation (λ = 1.54178 Å). All data were integrated with *SAINT* and a multiscan absorption correction using *SADABS* was applied.[43,44] The structure were solved by dual methods using *XT* and refined by full-matrix least-squares methods against F^2 by *XL*.[45,46] Structure solution and refinement cycles were performed within the graphical user interface of *OLEX2*.[47] Ellipsoids are drawn at the 50% probability level and hydrogen atoms are shown as sphere of arbitrary size. All electronic circular dichroism experiments were performed at 24 °C on a Jasco J-1500 spectrometer. Spectra were obtained in the specified solvent at 0.1 mM (either mQ water or PBS/iPrOH). Stock solutions in MeCN (10 mM) were first prepared and then diluted. The solutions were allowed to settle for 3 h before measurement.

Experimental Procedures and Spectroscopic Data. *General procedure A.* An amount of substrate (1.0 equiv) was dissolved in HCl (20.0 equiv, C = 4.0 M in dioxane) and the reaction was stirred at rt until TLC analysis indicated that the reaction had gone to completion. The solution was then concentrated under reduced pressure.

General procedure B. An amount of substrate (1.0 equiv) was dissolved in EtOH (C = 0.15 M) and H_2O was added (C = 0.15 M) followed by LiOH·H_2O (4.0 equiv) in one portion. The reaction was stirred at rt until TLC analysis indicated that the reaction had gone to completion. The mixture was then diluted with H_2O and CH_2Cl_2, and the layers were separated. The aqueous layer was washed once with CH_2Cl_2, then acidified to pH = 3−4 with a 10% w/w aqueous $KHSO_4$ solution. The aqueous layer was extracted three times with CH_2Cl_2. The organic layers were combined, dried over Na_2SO_4, filtered and concentrated under reduced pressure.

General procedure C. An amount of the amine (1.0−1.1 equiv) and the carboxylic acid (1.0 equiv) were dissolved in DMF (C = 0.2 M), and the solution was cooled to 0 °C. HOBt (2.4 equiv) and EDC (2.4 equiv) were added, and the solution was stirred until dissolution of the reagents. Then, Et_3N (11.4 μL, d = 0.726, 81.7 μmol, 4.3 equiv) was added, and the solution was stirred at 0 °C for 5 min, then was allowed to reach rt. The stirring was continued until ESI-MS analysis indicated that the reaction had gone to completion. The solvent was then removed under reduced pressure, and the residual oil was diluted with EtOAC and a saturated aqueous solution of $NaHCO_3$. The layers were separated, and the aqueous layer was extracted two times with EtOAc. The organic layers were combined, washed three times with a saturated aqueous solution of $NaHCO_3$, washed three times with water, washed one time with brine, dried over Na_2SO_4, filtered, and concentrated under reduced pressure.

tert-Butyl (S)-2-((R)-hydroxy((1R,2R)-2-((S)-2-((R)-hydroxy-((1R,2R)-2-(methoxycarbonyl)cyclopentyl)methyl)pyrrolidine-1-carbonyl)cyclopentyl)methyl)pyrrolidine-1-carboxylate ***14***. An amount of **3**[26] (74.0 mg, 226 μmol, 1.0 equiv) was submitted to general procedure A to afford **10** as a colorless oil (59.0 mg, qttve). The crude oil was engaged in the synthesis of **14** without further purification. An amount of **3**[26] (92.0 mg, 281 μmol, 1.0 equiv) was submitted to general procedure B to afford **11** as a colorless oil (88.0 mg, qttve). The crude oil was engaged in the synthesis of **14** without further purification. An amount of **10** (16.8 mg, 63.8 μmol, 1.0 equiv) and **11** (20.0 mg, 63.8 μmol, 1.0 equiv) were submitted to general procedure C. The crude oil was chromatographed over SiO_2 (100:0 to 0:100 hexanes/EtOAc) to afford **14** as a pale-yellow oil (26 mg, 78%). A sample was purified by preparative-HPLC for analytical study (Atlantid C18, 19 × 100 mm, 5 μm − flow: 21.6 mL/min − gradient: A: H_2O (+0.1% formic acid), B: MeCN. 0 min: 30% B, 1 min: 30% B, 10 min: 40% B, 11 min: 40% B 11.5 min: 30% B, 15 min: 30% B). *Rf* = 0.34 (100% EtOAc). $[\alpha]_D^{25}$ −147.5 (c 12.0 g/L, $CHCl_3$). ^{1}H NMR (400 MHz, $CDCl_3$) δ 4.16 (m, 1H), 4.02−3.72 (m, 3H), 3.67 (m,

https://doi.org/10.1021/acs.joc.3c02840
J. Org. Chem. 2024, 89, 4283−4293

4H), 3.60−3.32 (m, 2H), 3.25 (dt, *J* = 10.6, 7.0 Hz, 1H), 3.00 (m, 1.0H), 2.90 (m, 1H), 2.74 (q, *J* = 9.1 Hz, 1H), 2.68−2.60 (q, *J* = 10.2 Hz, 1H), 2.37 (tdd, *J* = 10.3, 9.1, 7.5 Hz, 1H), 2.26−2.13 (m, 1H), 2.09−1.48 (m, 20H), 1.44 (s, 9H). 13C{1H} NMR (101 MHz, $CDCl_3$) δ 178.0, 176.5, 155.1, 79.2, 76.4, 75.8, 61.2, 60.9, 52.1, 49.6, 48.7, 48.4, 47.7, 46.9, 45.5, 30.7, 30.6, 29.7, 29.2, 28.7, 28.6, 25.4, 25.2, 24.9, 24.7, 24.5, 24.3, 24.1. HRMS (ESI) for $C_{28}H_{46}N_2O_7$ $[M+H]^+$: Calc: 523.3378; Found: 523.3352, for $C_{28}H_{46}N_2O_7$ $[M+Na]^+$: Calc: 545.3197; Found: 545.3172. HPLC: 100% (98:2).

tert-Butyl (S)-2-((R)-hydroxy((1R,2R)-2-((S)-2-((R)-hydroxy((1R,2R)-2-((S)-2-((R)-hydroxy((1R,2R)-2-(methoxycarbonyl)cyclopentyl)methyl)pyrrolidine-1-carbonyl)cyclopentyl)methyl)pyrrolidine-1-carbonyl)cyclopentyl)methyl)pyrrolidine-1-carboxylate ***22***. An amount of **14** (36.0 mg, 68.9 μmol, 1.0 equiv) was submitted to general procedure A to afford **14a** as a colorless oil (30.0 mg, 95%). The crude oil was engaged in the synthesis of **22** without further purification. An amount of **14** (56.0 mg, 107 μmol, 1.0 equiv) was submitted to general procedure B to afford **14b** as a light-yellow oil (43.0 mg, 79%). The crude oil was engaged in the synthesis of **22** without further purification. An amount of **14a** (24.0 mg, 52.4 μmol, 1.0 equiv) and **14b** (26.7 mg, 52.4 μmol, 1.0 equiv) were submitted to general procedure C. The crude oil was chromatographed over SiO_2 (100:0 to 95:5 CH_2Cl_2/MeOH) to afford **22** as a colorless oil (23.0 mg, 48%). A sample was purified by preparative-HPLC for analytical study (Xbridge C18, 19 × 100 mm, 5 μm − flow: 21.6 mL/min − gradient: A: H_2O (+0.1% formic acid), B: MeCN. 0 min: 40% B, 15 min: 40% B). *Rf* = 0.28 (95:5 CH_2Cl_2/MeOH). $[\alpha]_D^{25}$ −167.8 (*c* 8.0 g/L, $CHCl_3$). ^{1}H NMR (500 MHz, $CDCl_3$) δ 4.22−4.10 (m, 3H), 4.02−3.71 (m, 5H), 3.68 (s, 10H), 3.30−3.23 (m, 1H), 2.8 (m, 1H) 2.76−2.61 (m, 4H), 2.44−2.27 (m, 3H), 2.21−1.56 (m, 36H), 1.45 (s, 12H). 13C{1H} NMR (101 MHz, $CDCl_3$) δ 178.0, 176.4, 175.9, 175.5, 155.0, 79.1, 77.4, 76.5, 75.9, 75.9, 75.7, 61.3, 61.2, 61.1, 60.9, 52.1, 50.1, 49.7, 48.9, 48.5, 48.3, 48.2, 47.6, 47.0, 45.4, 45.3, 30.6, 30.4, 30.2, 30.1, 29.8, 29.6, 29.2, 29.0, 29.0, 28.8, 25.5, 25.4, 25.4, 25.3, 25.0, 24.8, 24.6, 24.3, 24.3, 23.8, 23.3, 23.3. HRMS (ESI) for $C_{50}H_{80}N_4O_{11}$ $[M+H]^+$: Calc: 913.5896; Found: 913.5885, for $C_{50}H_{80}N_4O_{11}$ $[M+Na]^+$: Calc: 935.5716; Found: 935.5709. HPLC: 98% (98:1:1).

(1R,2R)-2-((R)-Hydroxy((S)-1-((1R,2R)-2-((R)-hydroxy((S)-pyrrolidin-2-yl)methyl)cyclopentane-1-carbonyl)pyrrolidin-2-yl)methyl)-cyclopentane-1-carboxylic acid hydrochloride ***18***. An amount of **14b** (8.8 mg, 17.2 μmol, 1.0 equiv) was submitted to general procedure A to afford **18** as a colorless oil (4.6 mg, 60%). A sample was purified by preparative-HPLC for analytical study (SunFire C18, 19 × 100 mm, 5 μm − flow: 21.6 mL/min − gradient: A: H_2O (+0.1% formic acid), B: MeOH. 0 min: 0% B, 1 min: 0% B, 10 min: 30% B, 11 min: 30% B 11.5 min: 0% B, 15 min: 0% B). *Rf* = 0.4 (50:50 CH_2Cl_2/MeOH). $[\alpha]_D^{25}$ −76.7 (*c* 3.0 g/L, MeOH). ^{1}H NMR (700 MHz, CD_3OD) δ 4.61 (bs, 1H), 4.16 (m, 0.9H), 4.05 (m, 0.1H) 3.94 (d, *J* = 9.9 Hz, 0.9H), 3.90 (m, 0.1H) 3.81 (m, 0.9H), 3.75 (m, 0.1H), 3.71 (dd, *J* = 8.7, 3.7 Hz, 0.9H), 3.56 (m, 1H), 3.47 (m, 1H), 3.27 (m, 2H), 2.98 (m, 1H), 2.70 (m, 1H), 2.50 (m, 0.1H) 2.46−2.38 (p, *J* = 4.7 Hz, 1H), 2.25 (m, 1H), 2.13−1.79 (m, 13H), 1.78−1.64 (m, 5H), 1.58−1.49 (m, 1H), 1.43 (m, 1H). 13C{1H} NMR (101 MHz, CD_3OD) δ 180.5, 177.2, 75.8, 75.5, 73.4, 64.6, 62.1, 62.1, 49.8, 49.3, 48.9, 48.2, 48.0, 47.3, 47.3, 46.7, 32.1, 31.9, 31.7, 30.7, 30.5, 30.3, 26.6, 26.4, 26.1, 26.0, 24.6, 24.5, 24.4. HRMS (ESI) for $C_{22}H_{36}N_2O_5$ $[M+H]^+$: Calc: 409.2697; Found: 409.2698. HPLC: 98% (98:2).

tert-Butyl (S)-2-((R)-hydroxy((1S,2S)-2-((S)-2-((R)-hydroxy((1S,2S)-2-(methoxycarbonyl)cyclopentyl)methyl)pyrrolidine-1-carbonyl)cyclopentyl)methyl)pyrrolidine-1-carboxylate ***15***. An amount of **4**[26] (100 mg, 305 μmol, 1.0 equiv) was submitted to general procedure A to afford **4a** as a colorless oil (80.0 mg, qttve). The crude oil was engaged in the synthesis of **15** without further purification. An amount of **4**[26] (90.0 mg, 275 μmol, 1.0 equiv) was submitted to general procedure B to afford **4b** as a colorless oil (84.0 mg, qttve). The crude oil was engaged in the synthesis of **15** without further purification. An amount of **4a** (48.5 mg, 185 μmol, 1.0 equiv) and **4b** (59.0 mg, 188 μmol, 1.02 equiv) were submitted to general procedure C. The crude oil was chromatographed over SiO_2 (100:0 to 0:100 hexanes/EtOAc) to afford **15** as a pale-yellow oil (70.0 mg, 73%). A sample was purified by preparative-HPLC for analytical study (Atlantid C18, 19 × 100 mm, 5 μm − flow: 21.6 mL/min − gradient: A: H_2O (+0.1% formic acid), B: MeOH. 0 min: 40% B, 1 min: 40% B, 10 min: 70% B, 11 min: 70% B 11.5 min: 40% B, 15 min: 40% B). *Rf* = 0.31 (100% EtOAc). $[\alpha]_D^{25}$ −2.9 (*c* 17.0 g/L, $CHCl_3$). ^{1}H NMR (400 MHz, $CDCl_3$) δ 5.15−4.87 (bs, 1H), 4.27 (ddd, *J* = 7.8, 5.6, 1.9 Hz, 1H), 3.93 (m, 1H), 3.82 (dd, *J* = 4.8, 2.0 Hz, 1H), 3.73 (m, 1H), 3.65 (s, 3H), 3.64−3.44 (m, 3H), 3.21 (dt, *J* = 10.7, 6.8 Hz, 1H), 2.82 (m, 2H), 2.46 (m, 1H), 2.26 (m, 1H), 2.04−1.51 (m, 20H), 1.45 (s, 9H). 13C{1H} NMR (176 MHz, $CDCl_3$) δ 177.2, 176.6, 156.9, 80.3, 74.5, 74.4, 62.6, 62.5, 51.8, 48.7, 48.2, 47.8, 47.2, 45.6, 45.2, 30.5, 29.6, 28.6, 27.4, 27.0, 26.7, 25.8, 25.6, 25.4, 24.9, 24.6. HRMS (ESI) for $C_{28}H_{46}N_2O_7$ $[M+H]^+$: Calc: 523.3378; Found: 523.3387, for $C_{28}H_{46}N_2O_7$ $[M+Na]^+$: Calc: 545.3197; Found: 545.3208. HPLC: 100%.

tert-Butyl (S)-2-((R)-hydroxy((1S,2S)-2-((S)-2-((R)-hydroxy((1S,2S)-2-((S)-2-((R)-hydroxy((1S,2S)-2-(methoxycarbonyl)cyclopentyl)methyl)pyrrolidine-1-carbonyl)cyclopentyl)methyl)pyrrolidine-1-carbonyl)cyclopentyl)methyl)pyrrolidine-1-carboxylate ***23***. An amount of **15** (30.0 mg, 57.4 μmol, 1.0 equiv) was submitted to general procedure A to afford **15a** as a colorless oil (25.0 mg, 95%). The crude oil was engaged in the synthesis of **23** without further purification. An amount of **15** (29.0 mg, 55.5 μmol, 1.0 equiv) was submitted to general procedure B to afford **15b** as a light-yellow oil (25.0 mg, 89%). The crude oil was engaged in the synthesis of **23** without further purification. An amount of **15a** (18.0 mg, 39.3 μmol, 1.0 equiv) and **15b** (20.0 mg, 39.3 μmol, 1.0 equiv) were submitted to general procedure C. The crude oil was chromatographed over SiO_2 (100:0 to 95:5 CH_2Cl_2/MeOH) to afford **23** as a colorless oil (26.0 mg, 72%). A sample was purified by preparative-HPLC for analytical study (Xbridge C18, 19 × 100 mm, 5 μm − flow: 21.6 mL/min − gradient: A: H_2O (+0.1% formic acid), B: MeCN. 0 min: 45% B, 15 min: 45% B). *Rf* = 0.28 (95:5 CH_2Cl_2/MeOH). $[\alpha]_D^{25}$ +16.7 (*c* 14.0 g/L, $CHCl_3$). ^{1}H NMR (500 MHz, $CDCl_3$) δ 4.82 (m, 2H), 4.30−4.24 (m, 1H), 4.12−4.03 (m, 2H), 3.97 (bs, 1H), 3.90−3.80 (m, 4H), 3.65 (m, 4H), 3.62−3.43 (m, 6H), 3.27−3.17 (m, 1H), 2.89−2.75 (m, 4H) 2.43−2.39 (m, 1H), 2.37−2.28 (m, 1H), 2.29−2.21 (m, 2H), 2.08−1.52 (m, 40H), 1.45 (s, 9H). 13C{1H} NMR (101 MHz, $CDCl_3$) δ 177.3, 176.0, 80.4, 77.5, 77.2, 76.8, 74.2, 62.8, 51.7, 48.7, 48.5, 47.8, 46.8, 45.6, 30.9, 30.0, 29.4, 28.7, 26.8, 25.9, 25.2, 25.1, 25.1.HRMS (ESI) for $C_{50}H_{80}N_4O_{11}$ $[M+H]^+$: Calc: 913.5896; Found: 913.5921, for $C_{50}H_{80}N_4O_{11}$ $[M+Na]^+$: Calc: 935.5716; Found: 935.5739. HPLC: 97%.

(1S,2S)-2-((R)-Hydroxy((S)-1-((1S,2S)-2-((R)-hydroxy((S)-pyrrolidin-2-yl)methyl)cyclopentane-1-carbonyl)pyrrolidin-2-yl)methyl)-cyclopentane-1-carboxylic acid hydrochloride ***19***. An amount of **15b** (15.0 mg, 29.5 μmol, 1.0 equiv) was submitted to general procedure A. The resulting oil was dissolved in a minimum amount of CH_2Cl_2 and Et_2O was added until **19** precipitated. The white solid was washed three times with Et_2O to afford **19** as a colorless oil (9.0 mg, 69%). A sample was purified by preparative-HPLC for analytical study (SunFire C18, 19 × 100 mm, 5 μm − flow: 21.6 mL/min − gradient: A: H_2O (+0.1% formic acid), B: MeCN. 0 min: 0% B, 1 min: 0% B, 10 min: 40% B, 11 min: 40% B 11.5 min: 0% B, 15 min: 0% B). *Rf* = 0.42 (90:10 CH_2Cl_2/MeOH). $[\alpha]_D^{25}$ +24.0 (*c* 9.0 g/L, MeOH). ^{1}H NMR (400 MHz, CD_3OD) δ 4.19 (bs, 1H), 3.76 (dd, *J* = 7.9, 3.3 Hz, 1H), 3.70 (dd, *J* = 7.4, 3.3 Hz, 1H), 3.60 (m, 2H), 3.47 (m, 1H), 3.27 (m, 2H), 2.74 (m, 1H), 2.40 (p, *J* = 8.5 Hz, 1H), 2.28 (t, *J* = 7.7 Hz, 1H), 2.13−1.55 (m, 20H). 13C{1H} NMR (101 MHz, CD_3OD) δ 176.1, 79.5, 79.2, 78.9, 74.9, 72.5, 65.0, 62.0, 49.1, 48.5, 47.9, 46.9, 31.7, 30.4, 29.4, 26.8, 25.6, 25.6, 25.4, 25.0, 24.8. HRMS (ESI) for $C_{22}H_{36}N_2O_5$ $[M+H]^+$: Calc: 409.2697; Found: 409.2702. HPLC: 100%.

tert-Butyl (S)-2-((S)-hydroxy((1S,2S)-2-((S)-2-((S)-hydroxy((1S,2S)-2-(methoxycarbonyl)cyclopentyl)methyl)pyrrolidine-1-carbonyl)cyclopentyl)methyl)pyrrolidine-1-carboxylate ***16***. An amount of **5**[26] (96.0 mg, 293 μmol, 1.0 equiv) was submitted to general procedure A to afford **5a** as a colorless oil (75.0 mg, 97%). The crude oil was

https://doi.org/10.1021/acs.joc.3c02840
J. Org. Chem. 2024, 89, 4283−4293

engaged in the synthesis of **16** without further purification. An amount of **5**[26] (95.0 mg, 290 μmol, 1.0 equiv) was submitted to general procedure B to afford **5b** as a colorless oil (90.0 mg, qttve). The crude oil was engaged in the synthesis of **16** without further purification. An amount of **5a** (48.5 mg, 185 μmol, 1.0 equiv) and **5b** (59.0 mg, 188 μmol, 1.02 equiv) were submitted to general procedure C. The crude oil was chromatographed over SiO_2 (100:0 to 0:100 hexanes/EtOAc) to afford **16** as a white foam (70.0 mg, 73%). A sample was purified by preparative-HPLC for analytical study (Atlantid C18, 19 × 100 mm, 5 μm − flow: 21.6 mL/min − gradient: A: H_2O (+0.1% formic acid), B: MeOH. 0 min: 40% B, 1 min: 40% B, 10 min: 90% B, 11 min: 90% B 11.5 min: 40% B, 15 min: 40% B). *Rf* = 0.35 (60:40 hexanes/EtOAc). $[\alpha]_D^{25}$ +8.4 (*c* 5.3 g/L, $CHCl_3$). ^1H NMR (400 MHz, $CDCl_3$) δ 5.03 (s, 2H), 4.17 (m, 1H), 3.65 (m, 6H), 3.50 (m, 1H), 3.47−3.35 (m, 2H), 3.31−3.23 (m, 1H), 3.11 (m, 1H), 3.01−2.93 (m, 1H), 2.63 (m, 1H), 2.41 (m, 1H), 2.02−1.54 (m, 20H), 1.45 (s, 9H). 13C{1H} NMR (101 MHz, $CDCl_3$) δ 179.6, 178.1, 158.6, 80.5, 78.1, 62.1, 61.8, 51.8, 48.2, 47.4, 46.7, 46.3, 43.3, 42.1, 42.1, 32.2, 32.0, 31.0, 30.9, 28.7, 28.6, 28.6, 26.1, 25.8, 24.4, 24.2. HRMS (ESI) for $C_{28}H_{46}N_2O_7$ $[M+H]^+$: Calc: 523.3378; Found: 523.3373, for $C_{28}H_{46}N_2O_7$ $[M+Na]^+$: Calc: 545.3197; Found: 545.3197. HPLC: 97%.

tert-Butyl (S)-2-((S)-hydroxy((1S,2S)-2-((S)-2-((S)-hydroxy((1S,2S)-2-((S)-2-((S)-hydroxy((1S,2S)-2-((S)-2-((S)-hydroxy((1S,2S)-2-(methoxycarbonyl)cyclopentyl)methyl)pyrrolidine-1-carbonyl)-cyclopentyl)methyl)pyrrolidine-1-carbonyl)cyclopentyl)methyl)-pyrrolidine-1-carbonyl)cyclopentyl)methyl)pyrrolidine-1-carboxylate ***24***. An amount of **16** (37.0 mg, 70.8 μmol, 1.0 equiv) was submitted to general procedure A. The crude oil was chromatographed over SiO_2 (100:0 to 88:12 CH_2Cl_2/MeOH) to afford **16a** as a colorless oil (18.0 mg, 56%). **16a** was engaged in the synthesis of **24** without further purification. An amount of **16** (38.0 mg, 72.7 μmol, 1.0 equiv) was submitted to general procedure B to afford **16b** as a light-yellow oil (36.0 mg, 97%). The crude oil was engaged in the synthesis of **24** without further purification. An amount of **16a** (8.7 mg, 19 μmol, 1.0 equiv) and **16b** (9.66 mg, 19.0 μmol, 1.0 equiv) were submitted to general procedure C. The crude oil was chromatographed over SiO_2 (100:0 to 95:5 CH_2Cl_2/MeOH) to afford **24** as a colorless oil (8.0 mg, 46%). A sample was purified by preparative-HPLC for analytical study (Xbridge C18, 19 × 100 mm, 5 μm − flow: 21.6 mL/min − gradient: A: H_2O (+0.1% formic acid), B: MeCN. 0 min: 50% B, 15 min: 50% B). *Rf* = 0.32 (95:5 CH_2Cl_2/MeOH). $[\alpha]_D^{25}$ +16.7 (*c* 5.0 g/L, $CHCl_3$). ^1H NMR (700 MHz, $CDCl_3$) δ 5.38 (m, 2H), 5.20−5.12 (m, 2H), 4.16 (m, 1H), 4.00 (m, 2H), 3.76 (m, 3H), 3.71−3.35 (m, 15H), 3.27 (m, 1H), 3.16 (m, 3H), 3.02−2.98 (m, 1H), 2.62 (m, 3H), 2.39 (m, 1H), 2.00−1.56 (m, 40H), 1.45 (s, 9H). 13C{1H} NMR (176 MHz, $CDCl_3$) δ 180.0, 179.7, 178.2, 158.6, 80.6, 77.7, 76.8, 62.7, 62.4, 61.9, 51.8, 48.2, 48.2, 47.4, 46.6, 46.5, 46.5, 46.1, 42.8, 42.0, 41.6, 41.5, 32.3, 32.2, 32.0, 31.1, 30.9, 28.6, 28.5, 28.3, 26.2, 26.0, 26.0, 25.7, 25.7, 25.6, 24.4, 24.4, 24.3, 24.3, 24.3. HRMS (ESI) for $C_{50}H_{80}N_4O_{11}$ $[M+H]^+$: Calc: 913.5896; Found: 913.5903, for $C_{50}H_{80}N_4O_{11}$ $[M+Na]^+$: Calc: 935.5716; Found: 935.5729. HPLC: 93% (98:1:1).

(1S,2S)-2-((S)-Hydroxy((S)-1-((1S,2S)-2-((S)-hydroxy((S)-pyrrolidin-2-yl)methyl)cyclopentane-1-carbonyl)pyrrolidin-2-yl)methyl)-cyclopentane-1-carboxylic acid hydrochloride ***20***. An amount of **16b** (18.0 mg, 35.4 μmol, 1.0 equiv) was submitted to general procedure A. The crude oil was chromatographed over SiO_2 (100:0 to 70:30 CH_2Cl_2/MeOH) to afford **20** as a colorless oil (15.2 mg, 97%). A sample was purified by preparative-HPLC for analytical study (Luna PFP, 19 × 100 mm, 5 μm − flow: 21.6 mL/min − gradient: A: H_2O (+0.1% formic acid), B: MeOH. 0 min: 0% B, 1 min: 0% B, 10 min: 40% B, 11 min: 40% B 11.5 min: 0% B, 15 min: 0% B). *Rf* = 0.4 (50:50 CH_2Cl_2/MeOH). $[\alpha]_D^{25}$ +12.4 (*c* 5.0 g/L, $CHCl_3$). ^1H NMR (700 MHz, CD_3OD) δ 4.34 (m, 0.75H), 4.27 (m, 0.25H), 3.74−3.60 (m, 2.6H), 3.55 (dt, *J* = 12.0, 7.7 Hz, 0.3H), 3.48−3.38 (m, 2H), 3.37−3.32 (m, 0.7H), 3.28−3.21 (m, 1.3H), 3.16 (q, *J* = 8.1 Hz, 0.25H), 3.05 (q, *J* = 8.7 Hz, 0.75H), 2.84 (m, 0.25H), 2.67 (q, *J* = 8.2 Hz, 0.75H), 2.51 (m, 0.75H), 2.44 (qd, *J* = 8.6, 3.0 Hz, 0.25H), 2.32 (p, *J* = 8.1 Hz, 0.75H), 2.21 (p, *J* = 8.8 Hz, 0.25H), 2.17 (m, 7H), 1.95−1.70 (m, 9H), 1.70−1.53 (m, 4H), 1.44 (m, 1H). 13C{1H} NMR (176 MHz, CD_3OD) δ 182.9, 180.1, 178.9, 81.9, 74.2, 74.0, 73.2, 64.9, 64.8, 63.1, 61.0, 50.2, 49.5, 48.6, 48.1, 48.0, 47.2, 46.9, 46.7, 46.2, 45.0, 33.6, 33.4, 32.3, 32.0, 31.9, 31.8, 30.9, 30.9, 30.4, 29.4, 28.4, 28.3, 26.7, 26.2, 26.1, 25.2, 25.2, 24.8, 23.1. HRMS (ESI) for $C_{22}H_{36}N_2O_5$ $[M+H]^+$: Calc: 409.2697; Found: 409.2712. HPLC: 100%.

tert-Butyl (S)-2-((S)-hydroxy((1R,2R)-2-((S)-2-((S)-hydroxy-((1R,2R)-2-(methoxycarbonyl)cyclopentyl)methyl)pyrrolidine-1-carbonyl)cyclopentyl)methyl)pyrrolidine-1-carboxylate ***17***. An amount of **6**[26] (80.0 mg, 244 μmol, 1.0 equiv) was submitted to general procedure A to afford **6a** as a colorless oil (64.0 mg, qttve). The crude oil was engaged in the synthesis of **17** without further purification. An amount of **6**[26] (80.0 mg, 244 μmol, 1.0 equiv) was submitted to general procedure B to afford **6b** as a colorless oil (76 mg, qttve). The crude oil was engaged in the synthesis of **17** without further purification. An amount of **6a** (47.2 mg, 180 μmol, 1.0 equiv) and **6b** (56.3 mg, 180 μmol, 1.0 equiv) were submitted to general procedure C. The crude oil was chromatographed over SiO_2 (100:0 to 90:10 hexanes/*i*-PrOH) to afford **17** as a white solid (74 mg, 79%). A sample was recrystallized by slow evaporation of $CHCl_3$. A sample was purified by preparative-HPLC for analytical study (Atlantid C18, 19 × 100 mm, 5 μm − flow: 21.6 mL/min − gradient: A: H_2O (+0.1% formic acid), B: MeCN. 0 min: 30% B, 1 min: 30% B, 10 min: 40% B, 11 min: 40% B 11.5 min: 30% B, 15 min: 30% B). Melting point: 85 °C. *Rf* = 0.27 (9:1 hexanes/*i*-PrOH). $[\alpha]_D^{25}$ −109.9 (*c* 5.5 g/L, $CHCl_3$). ^1H NMR (400 MHz, $CDCl_3$) δ 5.31−5.15 (m, 2H), 4.19−4.10 (m, 1H), 3.83−3.67 (m, 2H), 3.63 (s, 3H), 3.59−3.51 (m, 1H), 3.45 (dd, *J* = 7.3, 5.0 Hz, 3H), 3.37 (d, *J* = 9.3 Hz, 1H), 3.20 (dt, *J* = 11.1, 6.3 Hz, 1H), 3.02 (d, *J* = 9.5 Hz, 1H), 2.90 (q, *J* = 8.5 Hz, 1H), 2.46−2.35 (m, 1H), 2.26−2.14 (m, 1H), 2.01−1.57 (m, 20H), 1.43 (s, 9H). 13C{1H} NMR (101 MHz, $CDCl_3$) δ 178.7, 177.1, 158.6, 80.7, 75.5, 75.2, 62.1, 61.9, 51.6, 47.5, 47.4, 46.6, 45.9, 45.9, 45.3, 30.9, 30.4, 28.5, 28.4, 27.7, 25.4, 24.8, 24.5, 24.4, 24.0, 23.5. HRMS (ESI) for $C_{28}H_{46}N_2O_7$ $[M+H]^+$: Calc: 523.3378; Found: 523.3373, for $C_{28}H_{46}N_2O_7$ $[M+Na]^+$: Calc: 545.3197; Found: 545.3203. HPLC: 100%.

tert-Butyl (S)-2-((S)-hydroxy((1R,2R)-2-((S)-2-((S)-hydroxy-((1R,2R)-2-((S)-2-((S)-hydroxy((1R,2R)-2-((S)-2-((S)-hydroxy((1R,2R)-2-(methoxycarbonyl)cyclopentyl)methyl)pyrrolidine-1-carbonyl)-cyclopentyl)methyl)pyrrolidine-1-carbonyl)cyclopentyl)methyl)-pyrrolidine-1-carbonyl)cyclopentyl)methyl)pyrrolidine-1-carboxylate ***25***. An amount of **17** (12.0 mg, 23 μmol, 1.0 equiv) was submitted to general procedure A. The crude was chromatographed over SiO_2 (100:0 to 85:15 CH_2Cl_2/MeOH) to afford **17a** (7.0 mg, 67%) as a colorless oil. **17a** was engaged in the synthesis of **25** without further purification. An amount of **17** (12.0 mg, 23 μmol, 1.0 equiv) was submitted to general procedure B. The crude was chromatographed over SiO_2 (100:0 to 95:5 CH_2Cl_2/MeOH) to afford **17b** as a colorless oil (9 mg, 77%). **17b** was engaged in the synthesis of **25** without further purification. An amount of **17a** (7.0 mg, 15.4 μmol, 1.1 equiv) and **17b** (7.1 mg, 14.0 μmol, 1.0 equiv) were submitted to general procedure C. The crude oil was chromatographed over SiO_2 (100:0 to 95:5 CH_2Cl_2/MeOH) to afford **25** as a white powder (7.0 mg, 55%). A sample was purified by preparative-HPLC for analytical study (Xbridge C18, 19 × 100 mm, 5 μm − flow: 21.6 mL/min − gradient: A: H_2O (+0.1% formic acid), B: MeCN. 0 min: 50% B, 15 min: 50% B). *Rf* = 0.25 (95:5 CH_2Cl_2/MeOH). $[\alpha]_D^{25}$ −254.0 (*c* 6.0 g/L, $CHCl_3$). ^1H NMR (700 MHz, $CDCl_3$) δ 5.52 (m, 1.5H), 5.28 (m, 1.5H), 4.14 (m, 3H), 3.85−3.69 (m, 4H), 3.65 (s, 3H), 3.58 (m, 1.5H), 3.41 (m, 6.5H), 3.23 (dt, *J* = 10.5, 6.4 Hz, 1H), 3.08−2.99 (m, 3H), 2.92 (q, *J* = 9.4, 9.0 Hz, 1H), 2.47−2.39 (m, 3H), 2.26−2.19 (m, 1H), 2.04−1.59 (m, 40H), 1.45 (s, 9H). 13C{1H} NMR (176 MHz, $CDCl_3$) δ 178.8, 178.7, 178.7, 177.2, 158.6, 80.8, 75.6, 75.3, 75.2, 62.5, 62.4, 62.1, 61.9, 51.7, 47.8, 47.8, 47.5, 47.4, 46.6, 46.0, 46.0, 45.8, 45.3, 45.3, 30.9, 30.9, 30.9, 30.4, 28.5, 27.8, 27.8, 27.8, 25.4, 24.9, 24.6, 24.6, 24.5, 24.4, 24.0, 23.6, 23.6. HRMS (ESI) for $C_{50}H_{80}N_4O_{11}$ $[M+H]^+$: Calc: 913.5896; Found: 913.5899, for $C_{50}H_{80}N_4O_{11}$ $[M+Na]^+$: Calc: 935.5716; Found: 935.5722. HPLC: 100% (92:7:1).

https://doi.org/10.1021/acs.joc.3c02840
J. Org. Chem. 2024, 89, 4283−4293

(1R,2R)-2-((S)-Hydroxy((S)-1-((1R,2R)-2-((S)-hydroxy((S)-pyrrolidin-2-yl)methyl)cyclopentane-1-carbonyl)pyrrolidin-2-yl)methyl)-cyclopentane-1-carboxylic acid hydrochloride **21**. An amount of **17b** (9.0 mg, 17.7 μmol, 1.0 equiv) was submitted to general procedure A. The resulting solid was washed three times with CH_2Cl_2 to afford **21** as a colorless oil. (7.7 mg, qttve). A sample was purified by preparative-HPLC for analytical study (SunFire C18, 19 × 100 mm, 5 μm − flow: 21.6 mL/min − gradient: A: H_2O (+0.1% formic acid), B: MeCN. 0 min: 0% B, 1 min: 0% B, 10 min: 30% B, 11 min: 30% B 11.5 min: 0% B, 15 min: 0% B). *Rf* = 0.4 (50:50 CH_2Cl_2/MeOH). $[\alpha]_D^{25}$ −36.0 (*c* 5.0 g/L, MeOH). ^{1}H NMR (700 MHz, CD_3OD) δ 4.23−4.18 (m, 0.25H), 3.98 (dd, *J* = 9.7, 6.4 Hz, 0.75H), 3.77 (dt, *J* = 10.4, 6.8 Hz, 0.25H), 3.67 (m, 0.25H), 3.60 (m, 2.75H), 3.54−3.47 (m, 1H), 3.43−3.37 (m, 1H), 3.24 (ddd, *J* = 8.2, 6.7, 2.3 Hz, 2H), 3.00−2.90 (m, 1H), 2.75 (m, 0.25H), 2.63 (m, 0.75H), 2.52−2.40 (m, 1H), 2.27 (m, 1H), 2.17−1.89 (m, 9H), 1.84−1.59 (m, 10H), 1.50 (dtd, *J* = 12.0, 9.5, 7.3 Hz, 1H). 13C{1H} NMR (176 MHz, CD_3OD) δ 179.1, 176.8, 76.4, 72.5, 72.1, 71.3, 65.5, 65.0, 63.3, 62.2, 47.6, 47.5, 47.4, 47.1, 46.9, 46.7, 46.5, 46.4, 46.2, 31.7, 31.6, 31.5, 31.0, 29.3, 28.5, 27.9, 27.8, 26.4, 26.3, 26.0, 25.5, 25.4, 25.3, 25.2, 24.9, 24.8, 24.7, 22.7. HRMS (ESI) for $C_{22}H_{36}N_2O_5$ $[M+H]^+$: Calc: 409.2697; Found: 409.2715. UPLC: 100% (97:1.5:1.5).

■ ASSOCIATED CONTENT

Data Availability Statement

The data underlying this study are available in the published article and its Supporting Information.

Supporting Information

The Supporting Information is available free of charge at https://pubs.acs.org/doi/10.1021/acs.joc.3c02840.

Synthetic schemes; NMR spectra with ^{1}H and ^{13}C assignments; HPLC/UPLC chromatograms; X-ray description of **17** (PDF)

FAIR data, including the primary NMR FID files, for compounds **14**−**17** (ZIP)

FAIR data, including the primary NMR FID files, for compounds **18**−**21** (ZIP)

FAIR data, including the primary NMR FID files, for compounds **22**−**25** (ZIP)

Accession Codes

CCDC 2308003 contains the supplementary crystallographic data for this paper. These data can be obtained free of charge via www.ccdc.cam.ac.uk/data_request/cif, or by emailing data_request@ccdc.cam.ac.uk, or by contacting The Cambridge Crystallographic Data Centre, 12 Union Road, Cambridge CB2 1EZ, UK; fax: +44 1223 336033.

■ AUTHOR INFORMATION

Corresponding Author

Stephen Hanessian − *Department of Chemistry, Université de Montréal, Montréal H2V 0B3 QC, Canada;* orcid.org/0000-0003-3582-6972; Email: stephen.hanessian@umontreal.ca

Authors

Jean-Baptiste Garsi − *Department of Chemistry, Université de Montréal, Montréal H2V 0B3 QC, Canada;* orcid.org/0000-0001-7023-3270

Pedro M. Aguiar − *Department of Chemistry, Université de Montréal, Montréal H2V 0B3 QC, Canada*

Gilles Berger − *Microbiology, Bioorganic and Macromolecular Chemistry Unit, Faculty of Pharmacy, Université Libre de Bruxelles, 1050 Brussels, Belgium*

Thierry Maris − *Department of Chemistry, Université de Montréal, Montréal H2V 0B3 QC, Canada;* orcid.org/0000-0001-9731-4046

Complete contact information is available at: https://pubs.acs.org/10.1021/acs.joc.3c02840

Notes

The authors declare no competing financial interest.

■ ACKNOWLEDGMENTS

The authors thank NSERC and the NSERC-Servier Chair program for financial assistance.

■ REFERENCES

(1) Kotch, F. W.; Raines, R. T. Self-Assembly of Synthetic Collagen Triple Helices. *Proc. Natl. Acad. Sci. U. S. A.* **2006**, *103*, 3028−3033.

(2) Bhowmick, M.; Fields, G. B. Stabilization of Collagen-Model, Triple-Helical Peptides for In Vitro and In Vivo Applications. In *Peptide Modifications to Increase Metabolic Stability and Activity - Methods in Molecular Biology*; Cudic, P., Ed.; Springer, 2013; Vol. *1081*, pp 167−194. .

(3) Fallas, J. A.; O'Leary, L. E. R.; Hartgerink, J. D. Synthetic Collagen Mimics: Self-Assembly of Homotrimers, Heterotrimers and Higher Order Structures. *Chem. Soc. Rev.* **2010**, *39*, 3510−3527.

(4) Mandelkern, L. Poly-L-Proline. In *Poly-α-Amino Acids*; Dekker: New York, 1967; pp 675−724.

(5) DeRider, M. L.; Wilkens, S. J.; Waddell, M. J.; Bretscher, L. E.; Weinhold, F.; Raines, R. T.; Markley, J. L. Collagen Stability: Insights from NMR Spectroscopic and Hybrid Density Functional Computational Investigations of the Effect of Electronegative Substituents on Prolyl Ring Conformations. *J. Am. Chem. Soc.* **2002**, *124*, 2497−2505.

(6) Hodges, J. A.; Raines, R. T. Energetics of an n → Π* Interaction That Impacts Protein Structure. *Org. Lett.* **2006**, *8*, 4695−4697.

(7) Horng, J.-C.; Raines, R. T. Stereoelectronic Effects on Polyproline Conformation. *Protein Sci.* **2006**, *15*, 74−83.

(8) Shoulders, M. D.; Raines, R. T. Collagen Structure and Stability. *Annu. Rev. Biochem.* **2009**, *78*, 929−958.

(9) Bella, J. Collagen Structure: New Tricks from a Very Old Dog. *Biochem. J.* **2016**, *473*, 1001−1025.

(10) Narwani, T. J.; Santuz, H.; Shinada, N.; Melarkode Vattekatte, A.; Ghouzam, Y.; Srinivasan, N.; Gelly, J.-C.; de Brevern, A. G. Recent Advances on Polyproline II. *Amino Acids* **2017**, *49*, 705−713.

(11) Kumar, P.; Bansal, M. Structural and Functional Analyses of PolyProline-II Helices in Globular Proteins. *J. Struct. Biol.* **2016**, *196*, 414−425.

(12) Adzhubei, A. A.; Sternberg, M. J. E. Left-Handed Polyproline II Helices Commonly Occur in Globular Proteins. *J. Mol. Biol.* **1993**, *229*, 472−493.

(13) Adzhubei, A. A.; Sternberg, M. J. E. Conservation of Polyproline II Helices in Homologous Proteins: Implications for Structure Prediction by Model Building. *Protein Sci.* **1994**, *3*, 2395−2410.

(14) Okuyama, K. Revisiting the Molecular Structure of Collagen. *Connect. Tissue Res.* **2008**, *49*, 299−310.

(15) Gelse, K.; Pöschl, E.; Aigner, T. Collagens - Structure, Function, and Biosynthesis. *Adv. Drug Delivery Rev.* **2003**, *55*, 1531−1546.

(16) Mayne, R.; Burgeson, R. E. *Structure and Function of Collagen Types*; Academic Press: United States, 1987. .

(17) San Antonio, J. D.; Jacenko, O.; Fertala, A.; Orgel, J. P.R.O. R. O. Collagen Structure-Function Mapping Informs Applications for Regenerative Medicine. *Bioengineering* **2021**, *8*, 1−23.

(18) Berisio, R.; Vitagliano, L.; Mazzarella, L.; Zagari, A. Crystal Structure of the Collagen Triple Helix Model [(Pro-Pro-Gly)10]3. *Protein Sci.* **2002**, *11*, 262−270.

(19) Rabanal, F.; Ludevid, M. D.; Pons, M.; Giralt, E. CD of Proline-rich Polypeptides: Application to the Study of the Repetitive Domain of Maize Glutelin-2. *Biopolymers* **1993**, *33*, 1019−1028.
(20) Benedetti, E.; Bavoso, A.; di Blasio, B.; Pavone, V.; Pedone, C.; Toniolo, C.; Bonora, G. M. Solid-state Geometry and Conformation of Linear, Diastereoisomeric Oligoprolines. *Biopolymers* **1983**, *22*, 305−317.
(21) Matsuzaki, T. The Crystal Structure of T-Butyloxycarbonyltetra-L-Proline Benzyl Ester. *Acta Crystallogr. - Sect. B* **1974**, *B30*, 1029−1036.
(22) Wilhelm, P.; Lewandowski, B.; Trapp, N.; Wennemers, H. A Crystal Structure of an Oligoproline PPII-Helix, at Last. *J. Am. Chem. Soc.* **2014**, *136*, 15829−15832.
(23) Dobitz, S.; Aronoff, M. R.; Wennemers, H. Oligoprolines as Molecular Entities for Controlling Distance in Biological and Material Sciences. *Acc. Chem. Res.* **2017**, *50*, 2420−2428.
(24) Bonger, K. M.; Kapoerchan, V. V.; Grotenbreg, G. M.; Van Koppen, C. J.; Timmers, C. M.; Van Der Marel, G. A.; Overkleeft, H. S. Oligoproline Helices as Structurally Defined Scaffolds for Oligomeric G Protein-Coupled Receptor Ligands. *Org. Biomol. Chem.* **2010**, *8*, 1881−1884.
(25) Berger, G.; Vilchis-Reyes, M.; Hanessian, S. Structural Properties and Stereochemically Distinct Folding Preferences of 4,5-Cis and Trans-Methano-L-Proline Oligomers: The Shortest Crystalline PPII-Type Helical Proline-Derived Tetramer. *Angew. Chemie - Int. Ed.* **2015**, *54*, 13268−13272.
(26) Garsi, J.-B.; Aguiar, P. M.; Hanessian, S. Design of Pseudodiproline Dimers as Mimetics of Pro-Pro Units: Stereocontrolled Synthesis, Configurational Relevance, and Structural Properties. *J. Org. Chem.* **2021**, *86* (23), 16834−16847.
(27) Garsi, J.-B.; Komjáti, B.; Cullia, G.; Fejes, I.; Sipos, M.; Sipos, Z.; Fördős, E.; Markacz, P.; Balázs, B.; Lancelot, N.; Berger, S.; Raimbaud, E.; Brown, D.; Vuillard, L.-M.; Haberkorn, L.; Cukier, C.; Szlávik, Z.; Hanessian, S. Targeting NOX2 via P47/Phox-P22/Phox Inhibition with Novel Triproline Mimetics. *ACS Med. Chem. Lett.* **2022**, *13*, 949−954.
(28) Berlicki, Ł.; Kaske, M.; Gutiérrez-Abad, R.; Bernhardt, G.; Illa, O.; Ortuno, R. M.; Cabrele, C.; Buschauer, A.; Reiser, O. Replacement of Thr32 and Gln34 in the C-Terminal Neuropeptide Y Fragment 25−36 by Cis-Cyclobutane and Cis-Cyclopentane B-Amino Acids Shifts Selectivity toward the Y4 Receptor. *J. Med. Chem.* **2013**, *56*, 8422−8431.
(29) Choi, S. H.; Guzei, I. A.; Spencer, L. C.; Gellman, S. H. Crystallographic Characterization of Helical Secondary Structures in 2:1 and 1:2 α/B-Peptides. *J. Am. Chem. Soc.* **2009**, *131*, 2917−2924.
(30) Yamazaki, N.; Demizu, Y.; Sato, Y.; Doi, M.; Kurihara, M. Helical Foldamer Containing a Combination of Cyclopentane-1,2-Diamine and 2,2-Dimethylmalonic Acid. *J. Org. Chem.* **2013**, *78*, 9991−9994.
(31) Zheng, H.; Botos, I.; Clausse, V.; Nikolayevskiy, H.; Rastede, E. E.; Fouz, M. F.; Mazur, S. J.; Appella, D. H. Conformational Constraints of Cyclopentane Peptide Nucleic Acids Facilitate Tunable Binding to DNA. *Nucleic Acids Res.* **2021**, *49*, 713−725.
(32) Vitagliano, L.; Berisio, R.; Mastrangelo, A.; Mazzarella, L.; Zagari, A. Preferred Proline Puckerings in Cis and Trans Peptide Groups: Implications for Collagen Stability. *Protein Sci.* **2001**, *10*, 2627−2632.
(33) Haasnoot, C. A. G.; de Leeuw, F. A. A. M.; Altona, C. The Relationship between Proton-Proton NMR Coupling Constants and Substituent Electronegativities-I. An Empirical Generalization of the Karplus Equation. *Tetrahedron* **1980**, *36*, 2783−2792.
(34) Adzhubei, A. A.; Sternberg, M. J. E.; Makarov, A. A. Polyproline-II Helix in Proteins: Structure and Function. *J. Mol. Biol.* **2013**, *425*, 2100−2132.
(35) Toal, S.; Schweitzer-Stenner, R. Local Order in the Unfolded State: Conformational Biases and Nearest Neighbor Interactions. *Biomolecules* **2014**, *4*, 725−773.
(36) Rath, A.; Davidson, A. R.; Deber, C. M. The Structure of "Unstructured" Regions in Peptides and Proteins: Role of the Polyproline II Helix in Protein Folding and Recognition. *Biopolymers* **2005**, *80*, 179−185.
(37) Bochicchio, B.; Tamburro, A. M. Polyproline II Structure in Proteins: Identification by Chiroptical Spectroscopies, Stability, and Functions. *Chirality* **2002**, *14*, 782−792.
(38) Lopes, J. L. S.; Miles, A. J.; Whitmore, L.; Wallace, B. A. CD PPII 1 - Distinct Circular Dichroism Spectroscopic Signatures of Polyproline II and Unordered Secondary Structures: Applications in Secondary Structure Analyses. *Protein Sci.* **2014**, *23* (12), 1765−1772.
(39) Kakinoki, S.; Hirano, Y.; Oka, M. On the Stability of Polyproline-I and II Structures of Proline Oligopeptides. *Polym. Bull.* **2005**, *53* (2), 109−115.
(40) Zanna, N.; Milli, L.; Del Secco, B.; Tomasini, C. Factors Affecting the Stabilization of Polyproline II Helices in a Hydrophobic Environment. *Org. Lett.* **2016**, *18*, 1662−1665.
(41) Kümin, M.; Sonntag, L. S.; Wennemers, H. Azidoproline Containing Helices: Stabilization of the Polyproline II Structure by a Functionalizable Group. *J. Am. Chem. Soc.* **2007**, *129*, 466−467.
(42) Maaßen, A.; Gebauer, J. M.; Theres Abraham, E.; Grimm, I.; Neudorfl, J.-M.; Kuhne, R.; Neundorf, I.; Baumann, U.; Schmalz, H.-G. Triple-Helix-Stabilizing Effects in Collagen Model Peptides Containing PPII-Helix-Preorganized Diproline Modules. *Angew. Chemie - Int. Ed.* **2020**, *59*, 5747−5755.
(43) *Bruker. SAINT*. Bruker AXS Inc.: Madison, Winsconsin, USA, 2013.
(44) Krause, L.; Herbst-Irmer, R.; Sheldrick, G. M.; Stalke, D. Comparison of Silver and Molybdenum Microfocus X-Ray Sources for Single-Crystal Structure Determination. *J. Appl. Crystallogr.* **2015**, *48*, 3−10.
(45) Sheldrick, G. M. SHELXT - Integrated Space-Group and Crystal-Structure Determination. *Acta Crystallogr. Sect. A Found. Crystallogr.* **2015**, *A71*, 3−8.
(46) Sheldrick, G. M. Crystal Structure Refinement with SHELXL. *Acta Crystallogr. Sect. C Struct. Chem.* **2015**, *C71*, 3−8.
(47) Dolomanov, O. V.; Bourhis, L. J.; Gildea, R. J.; Howard, J. A. K.; Puschmann, H. OLEX2: A Complete Structure Solution, Refinement and Analysis Program. *J. Appl. Crystallogr.* **2009**, *42*, 339−341.

https://doi.org/10.1021/acs.joc.3c02840
J. Org. Chem. 2024, 89, 4283−4293